Pressure Effects and Thermal Stability of Myosin Rods and Rod Minifilaments: Fluorescence and Circular Dichroism Studies†

Lan King,* Chi Chang Liu, and Rouh-Fang Lee

Department of Biochemistry, Chang Gung Medical College, Tao-Yuan, Taiwan, Republic of China

Received July 29, 1993; Revised Manuscript Received February 22, 1994®

ABSTRACT: In the present study hydrostatic pressure was applied upon both skeletal myosin rod molecules and rod minifilaments to learn more of the intra- and intermolecular interaction behavior of myosin. Applied pressure disassembled the rod minifilaments into individual rod molecules and dissociated each myosin rod molecule into two chains of α-helix. The dissociation and disassembly profiles of these systems were obtained by measuring their fluorescent anisotropy under pressure. The mid-disassembly pressure of rod minifilaments at 0.4 mg/mL concentration was 430–490 bar. However, dissociation of two helical strands of rod molecules occurred at a much higher pressure, with a mid-disassembly pressure of 1300 bar at this concentration. These results indicate that the intramolecular interactions occurring between two α-helical chains of a rod molecule are much more stable under pressure than the intermolecular interactions that occur among rod molecules in a minifilament. The regions in the rod molecules involved in filament assembly were investigated through usage of both the intrinsic fluorescence of tryptophan residues and the extrinsic fluorescence of 6-acryloyl-2-(dimethylamino)naphthalene (acrylodan) labeled cysteine residues. The blue spectral shifts upon minifilament formation suggest the participation of both light meromyosin (LMM) and subfragment-2 (S-2) regions of myosin rods in the filament formation. Profiles of thermal unfolding of myosin rod molecules and rod minifilaments were obtained by circular dichroism measurement. The multiple transitions exhibited upon unfolding profiles indicated the presence of more than one structural domain, each correlating with a cooperative transition. The domain transitional temperatures were found to be 1–4 °C higher for rods in minifilaments than those for rod molecules in a solution of similar ionic composition, indicating that all structural domains are involved in filament assembly. Furthermore, the domain transitional temperatures for rod molecules in a buffer containing 0.6 M NaCl were 6–8 °C higher than those for rod molecules in 5 mM sodium pyrophosphate buffer, suggesting that each structural domain of a rod molecule becomes stabilized at 0.6 M NaCl solution.

Myosin comprises two heavy chains. The N-terminal region of each heavy chain folds together with light chains in forming globular head regions termed subfragment 1 (S-1).[1] Each head contains both a site for ATP binding and hydrolysis and an actin-binding site. The rest of the heavy chains wrap together forming coiled-coil α-helices referred to as rods. This region contains the binding sites for assembly of myosin into thick filaments, the functional form of myosin in muscle (Harrington & Rogers, 1984). The rod portion of the myosin molecule may be separated from the globular heads by either limited chymotrypsin or papain proteolysis (Lowey et al., 1969). Subsequent digestion with either trypsin or chymotrypsin cleaves the rod into two subfragments: subfragment 2 (S-2), which is the soluble portion immediately adjacent to the heads, and light meromyosin (LMM), the C-terminal half of the rod, which is responsible for the rod's insolubility (Margossian & Lowey, 1982). There are two tryptophan residues in each chain of skeletal rod located at positions 532 and 617 (Maeda et al., 1987). This tryptophan-containing region is located in the LMM portion of the rod near the LMM–S-2 junction (Figure 1). The environmentally sensitive characteristics of tryptophan residues are utilized for monitoring the dissociation and disassembly of rod molecules and rod minifilaments, respectively.

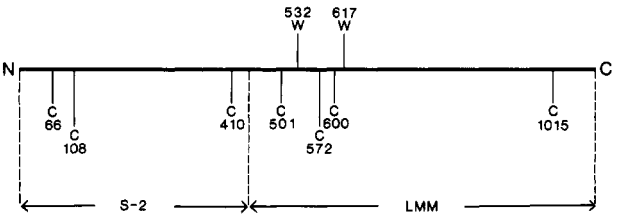

FIGURE 1: Location of tryptophan (W) and cysteine (C) residues on the chicken skeletal myosin rod.

The fluorescence emission spectra of some fluorophores, e.g., 6-propionyl-2-(dimethylamino)naphthalene (prodan) (Weber & Farris, 1979) and 6-acryloyl-2-(dimethylamino)-naphthalene (acrylodan) (Prendergast et al., 1983), are sensitive to a change in polarity of their surrounding environment. An increase of solvent polarity generally results in shifts of the emission spectrum toward longer wavelengths. These spectral red shifts are often accompanied by a decrease in fluorescence yield. The fluorescence emission spectrum of tryptophan is also apparently sensitive to solvent polarity. The tryptophan fluorescence spectral position of a protein may consequently be expected to be dependent upon the extent of exposure of its tryptophan residues to the aqueous phase (Lakowicz, 1983). Dissociation of the oligomeric protein may potentially result in a red shift of the emission spectrum due

† This work was supported by Chang Gung Medical Research Grant NMRP-B60 and National Science Council Research Grant NSC-81-042-B182-17 of Taiwan, Republic of China.

* Address for correspondence: Department of Biochemistry, Chang Gung Medical College, 259 Wen-Hwa One Road, Kwei-San, Tao-Yuan, Taiwan 33332, Republic of China.

® Abstract published in *Advance ACS Abstracts,* April 1, 1994.

[1] Abbreviations: acrylodan, 6-acryloyl-2-(dimethylamino)naphthalene; CD, circular dichroism; DTT, dithiothreitol; DTNB, 5,5′-dithiobis(2-nitrobenzoic acid); EDTA, ethylenediaminetetraacetic acid; LMM, light meromyosin; S-1, subfragment 1; S-2, subfragment 2; SDS, sodium dodecyl sulfate; Tris, tris(hydroxymethyl)aminomethane.

0006-2960/94/0433-5570$04.50/0

to the exposure of the tryptophan residues located at the interface between subunits into the aqueous phase. Additionally, the anisotropy of fluorescence provides information regarding the flexibility of the region to which the probe is attached. The motional freedom of the tryptophan residues trapped between subunits increases upon dissociation, consequently resulting in lower anisotropy values. Anisotropy values are therefore sensitive to the aggregation state of the oligomeric proteins. Dissociation of oligomeric proteins has been successfully monitored by following the decrease of their tryptophan fluorescence anisotropy (Xu & Weber, 1982; King & Weber, 1986; Ruan & Weber, 1988, 1993).

Application of hydrostatic pressure in the range from atmospheric pressure to 12 kbar upon solutions of pure proteins produces reversible effects that can be detected by changes in either absorption or emission of visible or ultraviolet light (Weber & Drickamer, 1983). A considerable number of single-chain proteins have already been investigated by this method [for review, see Heremans (1982) and Weber and Drickamer (1983)]. The profiles of the spectroscopic changes revealed, in most cases, a single spectral transition with a midpoint at 4–8 kbar, but almost no spectroscopic change has occurred at a pressure below 3 kbar. The reaction that leads toward a new conformation at a high pressure is being considered a "denaturation" and exhibits a correlation with other types of denaturations such as unfolding of the protein. A pressure below 3 kbar has been repeatedly shown to induce no detectable effect on the folding of single-chain proteins, which would validate the application of pressures below this limit for promoting dissociation of oligomeric proteins into minimally altered subunits. Restated, the pressure technique has the advantage of distinguishing between the dissociation (<3 kbar) and denaturation (>4 kbar) processes of oligomeric proteins by selecting a suitable pressure range, so as to produce folded subunits at a pressure below 3 kbar. Both heat and denaturant treatments are incapable of separating these two processes from each other. The reversible dissociation of oligomeric proteins by pressure below 3 kbar has been previously demonstrated in many systems [for review, see Weber (1987, 1991)].

The dissociation of tropomyosin into separated chains was previously demonstrated by the concentration dependence of its thermal-unfolding profiles (Holtzer et al., 1983). The possibility of chain dissociation of the skeletal myosin rod was also investigated by performing melting curves over a wide range of protein concentrations. The experimental curves did not reveal any concentration dependence as should be expected for a system in which dissociation occurs, strongly indicating that no chain dissociation occurred over a temperature range of 20–70 °C (Stafford, 1985).

In this paper, we demonstrate the dissociation of myosin rod into separated chains as a function of concentration and pressure by tryptophan fluorescence anisotropy changes. Furthermore, the participation of these tryptophan residues in the minifilament assembly has also been investigated. Therefore, tryptophan fluorescence anisotropy was applied to monitor the pressure-induced disassembly of rod minifilaments.

The conventional method employed in disassembling myosin filaments into individual myosin molecules involves raising the salt concentration to above 0.5 M. Most studies on the properties of the myosin molecule have been performed at such high salt solutions. However, the composition and the concentration of salt in solution affect the molecular structure and enzymatic activity of myosin (Warren et al., 1966), which underscores the inadequacy of studying thermodynamic equilibria of the assembly of myosin by changing the salt concentration, as well as the possible inaccuracy of the conformational information obtained as it may relate to its biological function. The pressure-induced disassembly of myosin filaments has been observed by the changes in the sedimentation constant or in the sedimentation equilibrium of myosin filaments as a function of centrifugal speed (Josephs & Harrington, 1967). However, the sedimentation observations in the ultracentrifuge are not useful for determining the thermodynamic properties under pressure in light of both the limited range of the pressure available and its variation along the sample cell. For this reason, tryptophan fluorescence anisotropy and scattering are utilized here to monitor the profile of pressure-induced disassembly of minifilaments to evaluate their thermodynamic properties.

Ionic interactions are apparently very important in the filament assembly in light of the high charge density at the α-helical coiled-coil surface (Davis, 1988). A model study based on sequence information has demonstrated a high degree of uniform intermolecular attraction throughout LMM, but almost no net attraction in the S-2 region (McLachlan & Karn, 1982, 1983). These findings are consistent with the idea that strong interactions between LMM regions occur in the core of the thick filaments, whereas the S-2 portion of rod can swing away from the filament surface as a result of its weak interactions (Huxley, 1969; Ueno & Harrington, 1981). A 5-kDa region near the C-terminus of LMM is responsible for the insolubility of LMM at low ionic strength as suggested from comparisons of the solubility of various proteolytic fragments (Nyitray et al., 1983). That small amino acid segment of LMM being critical for the solubility properties of LMM is confirmed by studies on the solubility profiles of a chicken gizzard LMM and its subfragments (Tashiro et al., 1985; Kumon et al., 1986; Cross & Vandekerckhove, 1986). Experiments using myosin demonstrated that deletion of a short peptide at the C-terminal end significantly increases its solubility in a low-ionic-strength buffer (Atkinson & Stewart, 1991), decreases aggregation (Maeda et al., 1991), and increases by 50-fold the critical concentration for the assembly of myosin rods into filaments (Hodge et al., 1992), while deletion of short segments at the N-terminus of the rod or of LMM produces only minor effects (Atkinson & Stewart, 1991; Hodge et al., 1992). Additionally, a nematode mutant, which is incapable of forming functional myosin filaments, has two amino acid changes (glycine for an arginine and lysine for a methionine) at the sixth and seventh residues from the amino terminus of the tail (Dibb et al., 1985). The defect in the mutant indicates that the head–tail junction must be involved in some interactions critical for filament assembly. No firm conclusion arises as to which portion of the rod is involved in the assembly of the thick filaments. Two additional approaches are therefore employed in this paper to determine the regions of rod molecules that participate in filament formation: (1) fluorescence probing technique; (2) domain stability. The former judges the participation of the probing region in the assembly, and the latter, the involvement of each structural domain in the assembly of thick filaments. In addition to the analysis of the intrinsic fluorescence of tryptophan residues, S-2 and LMM are selectively labeled with acrylodan to monitor the involvement of these regions in filament assembly.

MATERIALS AND METHODS

Protein Purification. Minced muscle tissue from chicken breast or rabbit back was extracted with 0.15 M sodium phosphate buffer, pH 7, containing 0.3 M NaCl, 1 mM EDTA,

and 1 mM DTT and filtered through six layers of cheese cloth. The filtrate was adjusted to 45 mM salt concentration for precipitating myosin (Sreter et al., 1972). The crude myosin was dissolved in 0.6 M NaCl, 1 mM EDTA, 1 mM DTT, and 50 mM sodium phosphate buffer, pH 7, and dialyzed against 70 mM NaCl, 1 mM EDTA, and 1 mM DTT in 30 mM phosphate buffer, pH 7. This step removed most of the contaminating proteins that are soluble at this ionic strength. The precipitate obtained after centrifugation was dissolved in 0.6 M NaCl, 1 mM EDTA, 1 mM DTT, and 50 mM sodium phosphate buffer, pH 7, and dialyzed against 0.12 M NaCl, 1 mM EDTA, and 1 mM DTT in 20 mM sodium phosphate buffer, pH 7, for chymotrypsin digestion.

Chicken (or rabbit) skeletal myosin rod was purified from the insoluble fraction (in 20 mM sodium phosphate buffer, pH 7, containing 40 mM NaCl, 1 mM EDTA, and 1 mM DTT) of a chymotryptic digest of myosin (Weeds and Pope, 1977). The crude rod was further purified by chromatography on a Bio-Gel A-15 (Bio-Rad) column. The purity of the samples was examined by SDS–polyacrylamide gel electrophoresis. The purified myosin rod sample was dialyzed against 0.6 M NaCl, 1 mM EDTA, 1 mM DTT, and 50 mM Tris-HCl buffer, pH 7.2, for pressure studies in light of the low pK dependency upon hydrostatic pressure (Neuman et al., 1973).

The preparation of chicken gizzard myosin was based on the method of Ebashi (1976). The only modification was the use of ammonium sulfate fractionation and column chromatography instead of the several high salt–low salt cycles. Gizzard myosin rod was prepared by papain digestion of myosin as described by Nath et al. (1986) and further purified by Bio-Gel A-15 (Bio-Rad) column chromatography. The fractions of pure rod were collected and concentrated to 3–5 mg/mL for fluorescence labeling.

Fluorescence Labeling. Seven cysteine residues are present in each chain of chicken skeletal rod, i.e., three in the S-2 region, at residues 66, 108, and 410, and the other four in the LMM region, at positions 501, 572, 600, and 1015 (Maita et al., 1991). The thiol groups in the LMM region are more reactive to acrylodan than those in the S-2 region. The S-2 region can be labeled selectively by blocking the more reactive thiol groups in LMM with 5,5′-dithiobis(2-nitrobenzoic acid) (DTNB).

The LMM portion of chicken skeletal myosin rod was labeled by reaction of 20 μM rod (completely reduced) with 0.6 mM of acrylodan (purchased from Molecular Probe) in 0.6 M NaCl/50 mM sodium phosphate buffer, pH 7, for 10 min at room temperature. The unreacted acrylodan and other possible impurities were removed by elution from a Bio-Gel A-15 column. The S-2 portion was labeled by complete blocking of the reactive thiol groups of the LMM portion with DTNB as follows: Myosin rod (25 μM) was reacted with DTNB (1 mM) for 2 h at room temperature, with the unreacted DTNB being removed by dialysis. The DTNB-treated rod was then reacted with acrylodan (0.75 mM) at room temperature for 30 min. The reaction was stopped by addition of 100 mM DTT, which also removed DTNB from the cysteine residue of rod molecules. The appropriate region of labeling was examined by either trypsin or chymotrypsin digestion; it was followed by separation of LMM and S-2 fragments by SDS–polyacrylamide gel electrophoresis. After completion, the gel was quickly placed on a UV box to examine the position of fluorescent bands. This was followed by Coomassie Brilliant Blue staining for identifying the fragments on the basis of molecular weight standards. The extent of probe perturbation of the structure was estimated by comparing the thermal unfolding profiles of labeled and native samples. Myosin rod molecules with an acrylodan-labeled LMM region have the first and second transition temperatures 1–2 °C lower than native rod molecules; meanwhile, rod molecules with an acrylodan-labeled S-2 region show almost no change at the transition temperatures (Table 3).

Table 1: Transition Pressures ($p_{1/2}$), Free Energies (ΔG), and Standard Volumes (ΔV) of Dissociation (Disassembly) of Skeletal Myosin Rods and Rod Minifilaments[a]

	$p_{1/2}$	ΔG	ΔV
chicken			
rod dissociation	1300	10.0	−90
minifilament disassembly	430	8.1	−60
rabbit			
rod dissociation	1300	11.0	−120
minifilament disassembly	490	8.4	−90

[a] Free energy in kilocalories/(mole of rods); volume in milliliters/(mole of rods); pressure in bars. Protein concentration is around 0.4 mg/ml.

Table 2: Average Fluorescence Wavelength (nm) of Myosin Rods and Rod Minifilaments

	chicken skeletal rods			gizzard rods
	native	acrylodan on S-2	acrylodan on LMM	acrylodan on Cys-43
rods in 0.6 M high salt	343.1	514.6	515.6	518.0
rods in 5 mM pyrophosphate	343.0	513.2	515.4	518.0
minifilaments in 5 mM pyrophosphate	341.0	509.1	510.6	515.5

No tryptophan residue is present in the gizzard myosin rod. The only cysteine residue (Cys-43) of each α-helical chain of gizzard myosin rod is labeled with acrylodan for monitoring possible participation of its surrounding region in filament formation. For this purpose, chicken gizzard myosin rod was reduced with 50 mM DTT at room temperature for 2 h to ensure complete reduction of the disulfide bond. It was followed by exhaustive dialysis for removal of all of the DTT. The labeling reaction was started immediately following dialysis so as to prevent reoxidation. It was carried out in 0.6 M NaCl, 1 mM EDTA, and 50 mM sodium phosphate solution, pH 7, in the presence of an excess amount of acrylodan (5:1 molar ratio) for 1 h at room temperature. Gizzard rods whose SH groups were completely blocked by DTNB were used as a control for verifying the specific labeling of acrylodan to SH groups. Unreacted acrylodan and impurities were removed by Bio-Gel A-15 (Bio-Rad) gel filtration. Fractions of pure acrylodan-labeled rod, as identified by the single fluorescent band upon polyacrylamide gel electrophoresis, were collected for fluorescence studies. Native gizzard rods and rod minifilaments exhibit thermal unfolding profiles indistinguishable from those of the acrylodan-labeled rods and rod minifilaments, suggesting that the attachment of acrylodan to the cysteine residue of a rod does not perturb its structure.

Rod Minifilaments. The high turbidity of filament was prevented from interfering with the spectroscopic measurements by utilizing rod minifilaments as an alternative for the filament state. Myosin rod minifilaments were prepared via a two-step dialysis procedure (Reisler et al., 1980, 1986). A soluble myosin rod in a low-ionic-strength buffer was produced by first dialyzing myosin rod (0.4–0.6 mg/mL) in 0.6 M NaCl and 50 mM sodium phosphate solution, pH 7.1, against 5 mM sodium pyrophosphate, pH 8, with several changes of fresh buffer. For pressure-induced disassembly studies, myosin rod

minifilaments were prepared by further dialyzing the soluble myosin rod in 5 mM sodium pyrophosphate, pH 8, against 10 mM citrate/Tris buffer, pH 7, at 25 °C. For thermal-unfolding studies, myosin rod minifilaments were prepared by further dialyzing the soluble myosin rod in 5 mM sodium pyrophosphate (pH 8) against 5 mM sodium pyrophosphate (pH 7.5 for gizzard rod minifilaments; pH 7 for chicken rod minifilaments). All solutions contained 1 mM EDTA and 1 mM DTT.

Circular Dichroism Measurements. Thermal Unfolding. Circular dichroism measurements were taken with an Aviv 60 DS spectropolarimeter (Lakewood, NJ) containing a Hewlett-Packard 89100A temperature controller which provided programmable sample temperature changes with 0.1 °C resolution. Ellipticity values at 222 nm, ranging from 25 to 70 °C, were measured using solutions in a stoppered, standard 1-cm Spectrosil quartz cuvette containing the temperature probe. The solution was stirred with a magnetic bar placed below the light path, enabling rapid temperature equilibration. Data were collected in 0.2 °C intervals using an equilibration time of 0.4 min and a data averaging time of 10 s at each temperature.

Fluorescence Measurements. Fluorescence measurements were carried out with an ISS K-2 fluorometer (Urbana, IL). All of the data were collected in the ratio mode. The intrinsic fluorescence of skeletal myosin rod is exclusively derived from tryptophan, as demonstrated by the coincidence of fluorescence spectra at 275- and 297-nm excitation. In light of the large scattering peak of rod molecules and rod minifilaments, a 280-nm excitation wavelength was chosen to minimize overlapping between scattering peak and fluorescence spectrum. The weighted average fluorescence wavelength, $\langle\lambda\rangle$, of intrinsic fluorescence was calculated with $\langle\lambda\rangle = [\sum\lambda F(\lambda)]/\sum F(\lambda)$ ranging from 290 to 460 nm in 1-nm steps using an ISS spectral analysis software program. The fluorescence anisotropy was measured using the L-format and an excitation wavelength of 280 nm with an excitation band pass of 8 nm. A WG-320 filter was placed in the emission light path to cut the scattering light. The fluorescence spectral analysis of acrylodan-labeled proteins was calculated from 400 to 660 nm in 1-nm increments using excitation at 375 nm. The method used is the same as that for the intrinsic spectral analysis. The technical spectrum was applied for all calculations.

Fluorescence Measurements under Pressure. Fluorescence measurements under pressure were carried out with an ISS K-2 fluorometer (Urbana, IL), which accommodates the high-pressure cell (ISS-NOVA). The weighted average fluorescence wavelength of intrinsic fluorescence was calculated with $\langle\lambda\rangle = [\sum\lambda F(\lambda)]/\sum F(\lambda)$ from 300 to 390 nm in 1-nm steps using excitation at 280 nm. The relative fluorescence yield was calculated as the area under the spectrum over the same wavelength range. The technical spectrum was applied for all analyses. The scattering intensity of rods and minifilaments at each pressure was calculated as the area under the scattering peak, which was measured from 265 to 295 nm in 1-nm steps using excitation at 280 nm. The fluorescence anisotropy was determined at 350 nm using the L-format and an excitation wavelength of 280 nm, with excitation and emission band passes of 8 and 16 nm, respectively. A WG-320 filter was placed in the emission light path for cutting the scattering light. The measurement of the anisotropy under pressure is rendered uncertain by the photoelastic birefringency of the windows of the pressure bomb (Paladini & Weber, 1981). A correction was therefore made by sets of pressure- and wavelength-dependent scrambling coefficients, which are calculated from the polarization spectra of a scattering solution (ficoll or glycogen), measured from atmospheric pressure to 3 kbar with 200-bar increments.

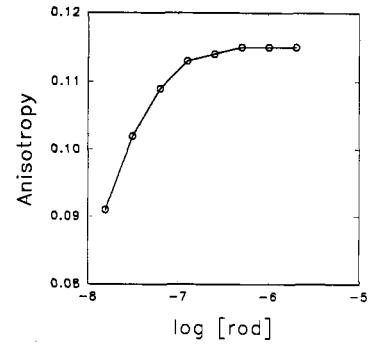

FIGURE 2: Concentration dependence of tryptophan fluorescence anisotropy of chicken skeletal myosin rods. Conditions for measurements are as follows: excitation at 280 nm with a band pass of 8 nm; emission filter WG-320.

Calculation and Simulation. The degree of dissociation of myosin rod, α, is defined as the fraction of rod that is dissociated into an individual α-helix strand. This α value can be calculated assuming a two-state transition and using the relationship

$$\alpha = [1 + Q^{-1}(A - A_M)/(A_D - A)]^{-1} \quad (1)$$

where A is the anisotropy of the fluorescence at a particular pressure, and A_D and A_M are the anisotropies of the fluorescence from pure dimer and monomer populations, respectively. $Q = Q_D/Q_M$, where Q_D and Q_M are proportional to the fluorescence yields of dimer and monomer, respectively.

The equilibrium constant of the dissociation is given by $K = 4C_0\alpha^2/(1 - \alpha)$, where C_0 is the total molar concentration of protein expressed as dimer. Consequently, the free energy of dissociation is calculated according to

$$\Delta G = -RT \ln K = -RT \ln[4C_0\alpha^2/(1-\alpha)] = -RT \ln C_0 - RT \ln[4\alpha^2/(1-\alpha)] \quad (2)$$

ΔG values are plotted against pressure, and least-squares calculations are used for determined $\Delta G°$ and m in the relationship

$$\Delta G = \Delta G° - mp \quad (3)$$

where $\Delta G°$ is the value of ΔG at atmospheric pressure (the intercept of the y axis), p is the pressure, and m is the slope of the straight line.

Combining eqs 2 and 3 yields

$$-RT \ln C_0 - RT \ln[4\alpha^2/(1-\alpha)] = \Delta G° - mp \quad (4)$$

The pressure dependence of the theoretical value of α can be generated by previously determined $\Delta G°$, m, and C_0 values. The theoretical α values, accompanied by A_D, A_M, and Q, are used for calculating the theoretical values of anisotropy by eq 1. Consequently, a simulated dissociation curve of myosin rod is produced (Figures 3 and 4). The standard volume change (ΔV) upon dissociation is derived from the equation

$$\Delta V = d\Delta G/dp = -RT\, d(\ln K)/dp = -RT\, d\{\ln[4\alpha^2/(1-\alpha)]\}/dp = RT[(2-\alpha)/\alpha(1-\alpha)](d\alpha/dp) \quad (5)$$

The disassembly process is also analyzed by a two-state assumption which has been previously suggested by the results

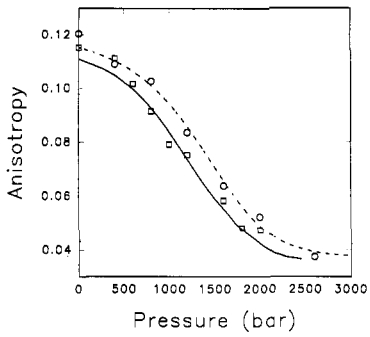

FIGURE 3: Pressure dependence of the tryptophan fluorescence anisotropy of chicken skeletal myosin rods at two different concentrations: 1.6×10^{-6} M (open circles) and 2.4×10^{-7} M (open squares). Conditions for measurements are as follows: excitation at 280 nm with a band pass of 8 nm; emission at 350 nm with a band pass of 16 nm; emission filter WG-320; temperature, 25 °C. Anisotropy values are corrected for the scrambling of the windows. Simulated curve of myosin rod at 1.6×10^{-6} M (- - -) and 2.4×10^{-7} M (—).

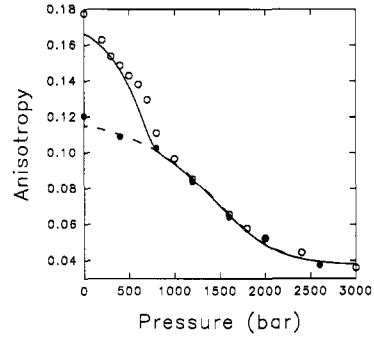

FIGURE 4: Pressure dependence of the tryptophan fluorescence anisotropy of chicken skeletal myosin rods (closed circles) and rod minifilaments (open circles). Conditions are the same as in Figure 3. Protein concentration is 1.6×10^{-6} M. Simulated curve of myosin rods (- - -) and rod minifilaments (—).

of sedimentation studies of myosin filaments (Josephs and Harrington, 1966). The degree of disassembly of rod minifilament into rod, β, is calculated by the same method as rod dissociation except that the equilibrium constant is given by $K = C_0^{n-1}(n\beta)^n/(1-\beta)$, where n is the number of rod molecules in a minifilament. However, a rod dissociation process occurs after the minifilament disassembly process. As a consequence, a general equation is applied as follows:

$$(\mathrm{D})_n \overset{\beta}{\rightleftharpoons} n\mathrm{D} \overset{\alpha}{\rightleftharpoons} 2n\mathrm{M}$$

where $(\mathrm{D})_n$ are minifilaments, D are intact rods (dimers), and M are dissociated rods (monomers). $(\mathrm{D})_n \rightleftharpoons n\mathrm{D}$ is the predominate process at low pressure (<600 bar) with $\mathrm{D} \rightleftharpoons 2\mathrm{M}$ being the predominate process at high pressure (>800 bar). Both processes have to be considered at medium pressure. The anisotropy observed, when all three species are present, is given by

$$A = [(1-\beta)Q_{(\mathrm{D})_n}A_{(\mathrm{D})_n} + \beta(1-\alpha)Q_{\mathrm{D}}A_{\mathrm{D}} + \alpha\beta Q_{\mathrm{M}}A_{\mathrm{M}}]/[(1-\beta)Q_{(\mathrm{D})_n} + \beta(1-\alpha)Q_{\mathrm{D}} + \alpha\beta Q_{\mathrm{M}}A_{\mathrm{M}}] \quad (6)$$

where β is the degree of disassembly of minifilaments into rod molecules and α is the degree of dissociation of rods into individual helix strands; $A_{(\mathrm{D})_n}$, A_{D}, and A_{M} are the anisotropies of minifilaments, intact rods (dimers), and dissociated rods (monomers), respectively; $Q_{(\mathrm{D})_n}$, Q_{D}, and Q_{M} are proportional to the fluorescence yields of minifilaments, intact rods (dimers), and dissociated rods (monomers), respectively. The pressure dependence of the theoretical values of α and β can be separately evaluated by the method described in the previous paragraph. The theoretical α and β values, accompanied by $A_{(\mathrm{D})_n}$, A_{D}, A_{M}, $Q_{(\mathrm{D})_n}$, Q_{D}, and Q_{M}, are used for calculating the theoretical anisotropy values by eq 6 so as to produce a disassembly–dissociation curve indicated by the solid line in Figure 4.

The scattering intensity data are processed by a similar method except for a slight modification as follows. The degree of dissociation of myosin rod, α, is calculated by assuming a two-state transition and applying the relationship

$$\alpha = [1 + 2(I - I_{\mathrm{M}})/(I_{\mathrm{D}} - I)]^{-1} \quad (7)$$

where I is the measured scattering intensity at a particular pressure, and I_{D} and I_{M} are the scattering intensities derived from pure dimer and monomer populations, respectively.

The degree of disassembly of rod minifilaments into rods, β, is calculated by the relationship

$$\beta = [1 + N(I - I_{\mathrm{D}})/(I_{(\mathrm{D})_n} - I)]^{-1}$$

where I is the measured scattering light intensity at a particular pressure; N is the number of rod molecules in minifilaments; and I_{D} and $I_{(\mathrm{D})_n}$ are the scattering light intensity of pure dimer and minifilament populations, respectively. A general equation is necessarily applied, since a rod dissociation process follows the minifilament disassembly process at a higher pressure; that is,

$$(\mathrm{D})_n \overset{\beta}{\rightleftharpoons} n\mathrm{D} \overset{\alpha}{\rightleftharpoons} 2n\mathrm{M}$$

The scattering intensity which is observed whenever all three species are present is

$$I = [(1-\beta)I_{(\mathrm{D})_n} + N\beta(1-\alpha)I_{\mathrm{D}} + 2N\alpha\beta I_{\mathrm{M}}]/[1 + (N-1)\beta + N\alpha\beta] \quad (8)$$

where β is the degree of disassembly of minifilaments into rod molecules; α is the degree of dissociation of rods into individual helix strands; and $I_{(\mathrm{D})_n}$, I_{D}, and I_{M} are the scattering intensities of minifilaments, intact rods (dimers), and dissociated rods (monomers), respectively.

RESULTS AND DISCUSSION

Pressure Dissociation of Myosin Rods

Both tryptophan residues (532 and 617) of skeletal myosin rods are located in "a" and "d" positions of a seven-residue (abcdefg) repeat of the coiled-coil structure. The amino acid residues in the "a" and "d" positions interlock with those of the other strand, forming a tight-fitting hydrophobic core. Dissociation of the two strands of the helix increases the motional freedom of these tryptophan residues as shown by a decrease in their anisotropy values. The following observations are considered as strong evidence for the validity of applying tryptophan fluorescence anisotropy toward monitoring the dissociation process of myosin rods:

(1) A pressure below 3 kbar has been repeatedly demonstrated to induce little effect upon the folding of single-chain proteins (Weber & Drickamer, 1983). Consequently, it would be reasonable to consider the change of spectral properties observed for an oligomeric protein at this pressure range as the result of dissociation of polypeptide chains rather than of

local unfolding. Dissociation of several oligomeric proteins under pressure has been successfully monitored by following the decrease of their tryptophan fluorescence anisotropy. The pressure dissociation profiles obtained by this method are consistent with those obtained by extrinsic probes monitoring the size of the aggregation states.

(2) Dilution is a common method that promotes the dissociation of oligomeric proteins. Tryptophan anisotropy of the myosin rod gradually decreases as the rod is being diluted to a concentration below 10^{-7} M. This concentration dependence of anisotropy validates the application of tryptophan anisotropy toward monitoring the dissociation of rod molecules.

(3) The anisotropy versus pressure curves (dissociation profiles) for myosin rods exhibit concentration dependence, as expected for a system in which dissociation occurs, strongly indicating that chain dissociation of rods actually occurs in this pressure range.

Concentration Dependence of Anisotropy. The tryptophan fluorescence anisotropy of chicken skeletal myosin rod was determined at various concentrations (Figure 2). As the protein was diluted, the anisotropy fell from a level of 0.115 at a concentration above 5×10^{-7} M to 0.091 at 1.6×10^{-8} M, which was the lowest concentration studied. A complete dissociation curve of rods by the dilution method was unsuccessful in light of the fact that the anisotropy for concentrations below 10^{-8} M cannot be accurately determined. However, the decrease of anisotropy upon dilution validates the application of this parameter toward monitoring the dissociation of two α-helical chains of rods.

Pressure Dependence of Anisotropy. The pressure dependence of the tryptophan fluorescence anisotropy of chicken skeletal rods at two different concentrations is illustrated in Figure 3. The anisotropy value decreases from 0.115 to 0.037 as the pressure increases from 1 bar to 2.6 kbar. The pressure of middissociation for rods at 1.6×10^{-6} M concentration was around 1.3 kbar, while that for rods at 2.4×10^{-7} M was around 1.1 kbar. Chain dissociation occurring over a pressure range from 1 bar to 2.6 kbar is clearly confirmed by the concentration dependence of anisotropy versus pressure profiles.

The reversibility of the pressure effect was determined by comparing the anisotropy values at equal pressures by raising the pressure in steps to above 2 kbar and in lowering it again in steps to atmospheric pressure. The difference in anisotropy values at each pressure is less than 5% at 2.4×10^{-7} M protein concentration and less than 2% at 1.6×10^{-6} M. Application of pressure did not induce aggregation within the 10-h time span of the experiment, as judged from the light-scattering intensity. The pressure dependency of anisotropy indicates a reversible two-state transition phenomenon inferred by its close correlation with the simulation curve obtained from the two-state assumption; i.e., the original particles and the dissociated products are characterized by constant anisotropy values (Figure 3). The pressure dependence of the degree of dissociation (α) for a chicken skeletal rod at 0.4 mg/mL is illustrated in Figure 5A. The $p_{1/2}$, at 50% dissociation ($\alpha = {}^1/_2$), was 1.3 kbar. The pressure dependence of the free energy of dissociation (ΔG) of chicken skeletal rods obtained from the two-state approximation is illustrated in Figure 6A. The value at atmospheric pressure was 10 kcal/(mol of rods), and the standard volume change upon dissociation (ΔV) was −90 mL/(mol of rods). The rabbit skeletal myosin rod produces results similar to those of the chicken skeletal rod (Table 1). The middissociation pressure was 1.3 kbar and is the same as

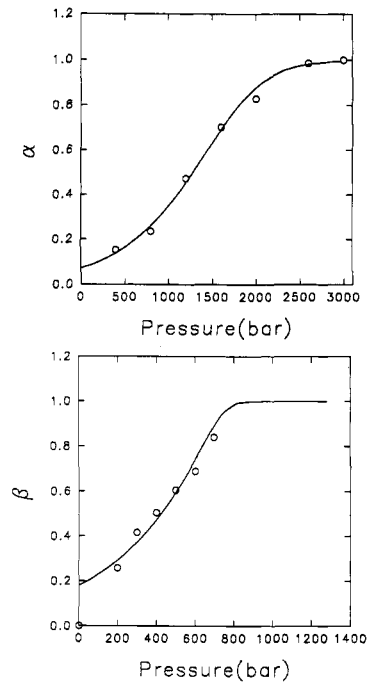

FIGURE 5: (A, top) Degree of dissociation of chicken skeletal myosin rods (α) versus pressure. The method for calculation of α from fluorescence anisotropy and the construction of simulated dissociation curves are described in Materials and Methods. (B, bottom) Degree of disassembly of chicken skeletal myosin rod minifilaments (β) versus pressure. Calculation of β from fluorescence anisotropy and the construction of the simulated disassembly curve are described in Materials and Methods.

that of chicken skeletal rod at an equivalent concentration. The standard free energy of dissociation at atmospheric pressure was 11 kcal/(mol of rods), and the standard volume change on dissociation was −120 mL/(mol of rods) (Table 1). Both the free energy of dissociation and the volume change on dissociation correlate with the data obtained for several other oligomeric proteins under pressure (Weber, 1993). The small volume change upon dissociation (only 1–2% of the volume of rod) suggests that the two α-helical chains of rod are tightly bonded to each other in the coiled-coil structure.

Fluorescence Spectrum. The fluorescence spectrum of chicken skeletal myosin rods exhibits an appreciable amount of red shift under pressure. The fluorescence spectra of chicken myosin rods at 1 bar and 2.7 kbar are shown in Figure 7. A clear red shift of the spectrum occurs at 2.7 kbar with an additional small flat shoulder observed at 430 nm at 2.7 kbar. This small flat shoulder is constantly observed with myosin rods, myosin, and rod minifilaments at a pressure above 1 kbar. The reason for this phenomenon remains unclear. The weighted average fluorescence wavelength has been calculated from 300 to 390 nm in order to minimize the interference of the additional shoulder at 430 nm at high pressure. The average wavelength of chicken myosin rods shifts from 340.7 nm at atmospheric pressure to 344.5 nm at 2.7 kbar. This red shift is significantly smaller than that of rod denatured in 6 M guanidine hydrochloride whose fluorescence spectrum is the same as that of tryptophan in water (351.3 nm). This result suggests that a pressure of 2.7 kbar did not unfold the rod molecule into a random coil. On the other hand, the red shift occurred at a pressure of approximately 1 kbar higher than that inducing anisotropy changes; in addition, the extent of red shift slowly increased as the incubation time under pressure increased, suggesting that the tryptophan residues are not immediately exposed to water upon dissociation. Restated, separation of two strands of the helix increases

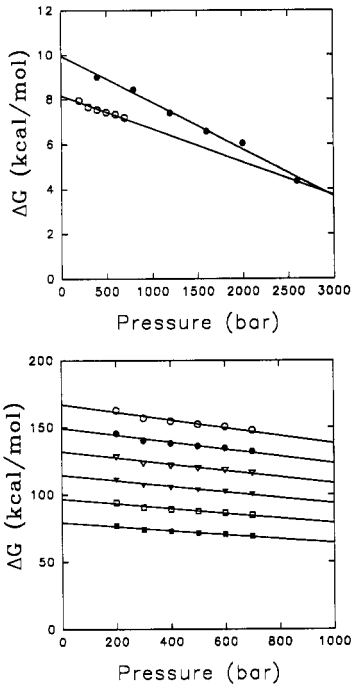

FIGURE 6: (A, top) Pressure dependence of the standard free energy change of dissociation of chicken skeletal myosin rods (●) and disassembly of rod minifilaments (○). The method of calculation is described in Materials and Methods. The free energy changes are presented as units of kilocalories/(mole of rod molecule). (B, bottom) Pressure dependence of the standard free energy change of disassembly of chicken skeletal myosin rod minifilaments. The method of calculation is described in Materials and Methods. The number of rod molecules in minifilaments is 10 (■), 12 (□), 14 (▲), 16 (△), 18 (●), 20 (○). The free energy changes are presented in units of kilocalories/(mole of rod minifilament).

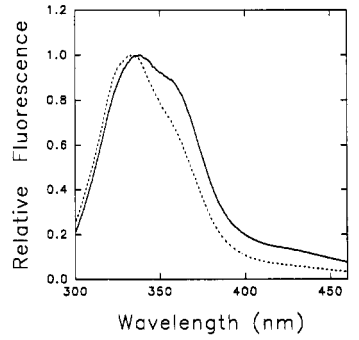

FIGURE 7: Normalized intrinsic fluorescence spectra of chicken skeletal myosin rods at 1 bar and 2.7 kbar. Myosin rods are dissolved in 0.6 M NaCl/50 mM Tris-HCl buffer, 1 mM DTT, and 1 mM EDTA, pH 7.2; (- - -) myosin rods at atmospheric pressure; (—) myosin rods at 2.7 kbar; excitation at 280 nm; band passes of 4 nm for both excitation and emission; temperature, 25 °C.

immediately the motional freedom of tryptophan residues; however, the adjustment of tryptophan residues into a polar aqueous environment is a much slower process. The dissociated monomer may possibly undergo slow and continuous conformational changes, i.e., conformation drift, a phenomenon also observed with other oligomeric proteins under pressure (Weber, 1986). Upon releasing the pressure to atmospheric pressure, the reassociated rod molecule is apparently incapable of maintaining its native conformation after having been incubated under pressure for several hours. The alteration of conformation of rod molecules being subjected to a pressure above 2 kbar for several hours is revealed by the change in the fluorescence spectrum (which resembles the spectrum under pressure) and the slow formation of aggregates in 0.6

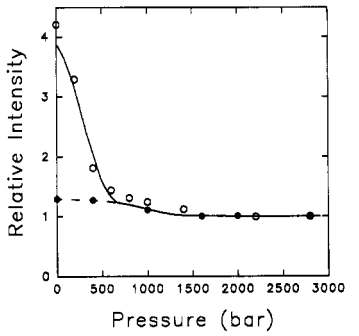

FIGURE 8: Pressure dependence of the light-scattering intensity of chicken skeletal myosin rods (●) and rod minifilaments (○). The scattering intensity of rods and minifilaments at each pressure is calculated as the area under the scattering peak measured from 265 to 295 nm in 1-nm steps using excitation at 280 nm with a band pass of 4 nm for both excitation and emission; temperature, 25 °C. Values exhibited at each pressure are normalized to the high-pressure value. Simulated curve of myosin rods (- - -) and rod minifilaments (—).

M high salt solution. The aggregation process was initiated from one to several days after pressure release, depending upon the pressure applied and its duration. The time dependence of the conformational change of the dissociated rod under pressure is being investigated so as to clarify the nature of the interaction between the two α-helical chains of the myosin rod.

Pressure Disassembly of Rod Minifilaments

The tryptophan residues of the myosin rod are relatively buried in the hydrophobic core, and their motional freedom is restricted in the coiled-coil structure. The neighboring rod molecules in minifilaments apparently provide an additional strain to the tryptophan residues and tend to further shield these tryptophan residues from exposure to the aqueous phase. This additional strain and the shielding effect are clearly demonstrated by the substantially higher anisotropy value of minifilaments (0.178) than that of soluble rods (0.120). The average fluorescence wavelength of minifilaments is also slightly shorter than for a rod molecule. The anisotropy value of rod minifilaments decreased from 0.178 to 0.036 as the pressure was increased from 1 bar to 3 kbar. The anisotropy of rod minifilaments subjected to pressure clearly indicates the occurrence of two successive processes. The break point of two distinct stages is around 800 bar. The second transition of minifilaments is primarily produced by the dissociation of the two α-helical chains of the rod molecule, as suggested from the coincidence of the profiles of rods (dotted line in Figure 4) and minifilaments (solid line in Figure 4) at a pressure greater than 1 kbar. Consequently, the first transition may correspond to the disassembly of rod minifilaments into rod molecules. This suggestion is confirmed by light-scattering studies under pressure.

The pressure dependence of the light scattering of chicken skeletal rods and rod minifilaments is shown in Figure 8. The scattering intensity of the rods decreases by roughly 20% as the pressure is increased from 1 bar to 1.6 kbar. No further changes arise in the scattering intensity as the pressure is raised from 1.6 to 2.8 kbar. The reversibility of the scattering intensity of myosin rods is greater than 90%. The scattering intensity of rod minifilaments decreases around 80% as the pressure increases from 1 bar to 2.2 kbar. The recovery of the scattering intensity is about 80% as the pressure is decreased, indicating that the minifilaments are not quite reassembled into the previous size and shape. The scattering intensity of rod minifilaments subjected to pressure indicates

two stages with a break point at roughly 700 bar. A disassembly process of minifilaments occurring in this transition is confirmed by the large decrease of scattering light intensity (approximately 65%) during the first transition. The second transition of minifilaments is primarily produced by the dissociation of rods into two chains of α-helix, as implied from the coincidence of the profiles of rods and minifilaments at a pressure greater than 1 kbar.

The occurrence of a disassembly process for minifilaments preceding rod dissociation is therefore specified by a comparison of the pressure dependence of the fluorescence anisotropy and scattering intensity of rods and rod minifilaments. The degree of disassembly, β, is estimated by an anisotropy value below 800 bar, assuming that the disassembly is the predominant process at this pressure range. The pressure dependence of the β value is illustrated in Figure 5B. The $p_{1/2}$, at which 50% of the disassembly ($\beta = {}^1/_2$) is observed, is 430 bar. This pressure value is substantially smaller than that for rod dissociation, suggesting that the intramolecular interactions within the rod molecule are significantly more stable under pressure than the intermolecular interactions taking place among rod molecules in minifilaments. The pressure dependence of the free energy of disassembly (ΔG) of rod minifilaments obtained from the two-state approximation is shown in Figure 6A,B. Various numbers ($N = 10$–20) are used for calculation since the numbers of rod molecules in minifilaments are unknown. The pressure dependence of the free energy of disassembly for conditions ranging from $N = 10$ to $N = 20$ is illustrated in Figure 6B. The values obtained for minifilaments of various sizes are proportional to the numbers of rod molecules. The value of the free energy of disassembly at atmospheric pressure is divided by the number of rod molecules in minifilaments (N) to obtain the free energy change of minifilament disassembly corresponding to each rod molecule, which is 8.1 kcal/(mol of rods) (Figure 6A). The standard volume change (ΔV) for the disassembly of chicken rod minifilaments is estimated to be –60 mL/(mol of rods).

Rabbit skeletal rod minifilaments produce results similar to those of chicken skeletal rod minifilaments. The middisassembly pressure for rabbit rod minifilaments is 490 bar, close to the value (430 bar) for chicken rod minifilaments at a comparable concentration. The standard free energy for disassembly of rabbit rod minifilaments at atmospheric pressure is 8.4 kcal/(mol of rods), which is similar to that of chicken rod minifilaments [8.1 kcal/(mol of rods)]. The standard volume of disassembly for rabbit rod minifilaments is estimated as being –90 mL/(mol of rods) (Table 1).

All calculations are based on a two-state assumption, as has been suggested by the results of equilibrium sedimentation studies of myosin filaments (Josephs & Harrington, 1966) and minifilaments (Oriol-Audit et al., 1981). Although myosin dimer has been observed under some solution conditions (Harrington & Burke, 1972; Davis et al., 1982; Reisler et al., 1986), simple two-state approximation apparently correlates reasonably well with the observed data. The standard volume changes calculated from our pressure disassembly profiles are less than those reported for rabbit myosin filaments [380 mL/(mol of myosin molecules)] in a previous study (Josephs & Harrington, 1968). Although the nature of assembly for rod minifilaments might not be precisely the same as for myosin filaments, the technique employed for determining the standard volume of disassembly may lead to a different value. The pressure reached in the equilibrium sedimentation studies of Josephs and Harrington was less than 100 bar, which is a considerable distance away from the midpoint of the disassembly transition (400–500 bar) estimated on the basis of our disassembly profiles. Therefore, Josephs and Harrington's calculation of volume change upon disassembly, based on the data obtained at an early stage of disassembly transition, may result in a different value. The small value of volume change according to our calculation suggests that the rod molecules are tightly packed in rod minifilaments.

In conclusion, our intrinsic fluorescence and scattering studies indicate that pressure disassemblies rod minifilaments into rod molecules and further dissociates an intact rod molecule into its subunits at a higher pressure. The intramolecular interactions between two chains of α-helix within coiled coils are substantially more stable under pressure than the intermolecular interactions among rod molecules in minifilaments.

Regions of Myosin Rods Participating in Filament Formation

Fluorescence Probing. Since intermolecular interactions affect the local environments of interacting regions by providing an additional strain and further shield from water molecules, the effect of assembly on the fluorescence properties of environmentally sensitive probes provides information regarding the region(s) of the rod involved in the formation of thick filaments. The average intrinsic fluorescence spectral position of chicken myosin rods in a phosphate buffer containing 0.6 M NaCl (high salt solution) is 343 nm, and the anisotropy in this solution is 0.115. These values did not change when the rod in high salt solution was dialyzed into 5 mM sodium pyrophosphate, pH 8 (Table 2). The local structure surrounding the tryptophan residues in the rod is apparently not affected by this range of variation in ionic strength as this is suggested by an identical fluorescence spectrum and anisotropy. The average fluorescence wavelength shifts from 343 to 341 nm (Table 2) and the anisotropy value increases 50% (Figure 4) upon the formation of minifilaments by changing the pH of 5 mM pyrophosphate buffer from 8 to 7. The involvement of the tryptophan-containing region (N-terminal region of LMM) in rod–rod interactions within a minifilament is clearly demonstrated by these results since no spectral shift and anisotropy change were observed by changing the pH value from 7 to 8 of rods in 0.6 M high salt buffer. Control experiments regarding pH variations in a high salt solution and the ionic strength variation from 0.6 M high salt solution to 5 mM pyrophosphate solution were also performed with acrylodan-labeled rods to exclude the possibility that the changes in fluorescence properties are due to local structural perturbations other than the probes being directly involved in filament assembly.

The average fluorescence spectral position of rods with an acrylodan-labeled LMM region shifts from 515.6 to 510.6 nm upon filament formation (Table 2), indicating involvement of the LMM region in the filament assembly. The average acrylodan fluorescence spectral position of S-2-labeled rods shifts from 514.6 to 509.1 nm after filament assembly (Table 2), which indicates that the S-2 region is also involved in filament formation. Our studies with probes on either the S-2 or LMM region can only determined whether the region is involved in filament association or not. Labeling one specific cysteine residue out of seven with acrylodan requires sophisticated labeling skill and has not yet been accomplished.

The fluorescence spectrum of acrylodan-labeled gizzard rods shifts from 518 to 515.5 nm upon minifilament formation (Table 2). This spectral blue shift of the acrylodan-labeled

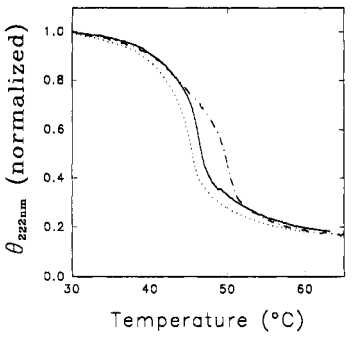

FIGURE 9: Normalized thermal helix unfolding profiles of chicken skeletal myosin rods with acrylodan label on S-2 portion: (···) myosin rods in 5 mM sodium pyrophosphate solution, pH 8, containing 1 mM EDTA and 1 mM DTT; (—) myosin rod minifilaments in 5 mM sodium pyrophosphate buffer, pH 7, containing 1 mM EDTA and 1 mM DTT; (– · –) myosin rods in 50 mM sodium phosphate solution, pH 7.1, containing 0.6 M NaCl, 1 mM EDTA, and 1 mM DTT.

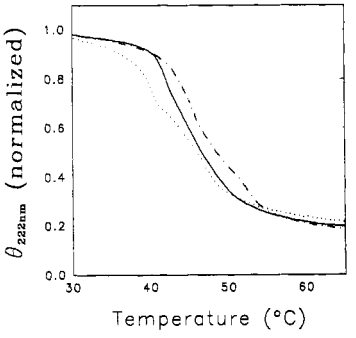

FIGURE 10: Normalized thermal helix unfolding profiles of rabbit skeletal myosin rods in different solutions: (···) myosin rods in 5 mM sodium pyrophosphate solution, pH 8, containing 1 mM EDTA and 1 mM DTT; (—) myosin rod minifilaments in 5 mM sodium pyrophosphate buffer, pH 7, containing 1 mM EDTA and 1 mM DTT; (– · –) myosin rods in 50 mM sodium phosphate solution, pH 7.1, containing 0.6 M NaCl, 1 mM EDTA, and 1 mM DTT.

cysteine residue (Cys-43) near the rod–head junction indicates that even the rod–head junction region is involved in filament assembly. This result is in agreement with the result obtained on a nematode mutant bearing two amino acid changes in the sixth and seventh residues from the rod N-terminus and which is incapable of forming filaments (Dibb et al., 1985).

Domain Stability. Skeletal myosin rods exhibit multiple temperature- and denaturant-induced unfolding transitions which involve regions of different stabilities (Burke et al., 1973; Goodno et al., 1976; Privalov, 1982; Cross et al., 1984; Stafford, 1985; King & Lehrer, 1988, 1989). Unfolding profiles of gizzard smooth myosin rods also exhibit two thermal and denaturant-induced cooperative transitions, indicating the presence of two major structural domains (King et al., 1989). How the stability of these domains is affected by the formation of filaments was examined here by comparing the circular dichroism (CD) unfolding profiles of myosin rods in a soluble and filamentous state. The effect of ionic strength on the thermal stability of myosin rods was also examined by the same method.

As shown in Figure 9 and Table 3, three thermal unfolding transitions occur in chicken skeletal rods. The transition midpoints for rods in 0.6 M NaCl solution are 44, 51, and 55 °C. However, myosin rods in 5 mM sodium pyrophosphate, pH 8, have transition midpoints at 38, 45, and 49 °C (Figure 9 and Table 3). It is suggested from the 5–6 °C shifts of the transition temperatures that high salt can stabilize each structural domain of the chicken skeletal rod. On the other hand, minifilament formation also stabilizes each structural

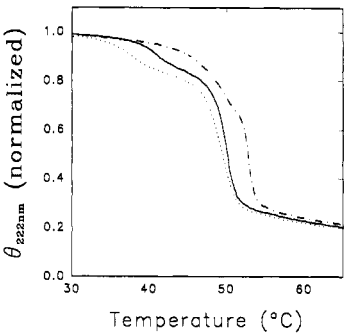

FIGURE 11: Normalized thermal helix unfolding profiles of acrylodan-labeled gizzard myosin rods in different solutions: (···) myosin rods in 5 mM sodium pyrophosphate solution, pH 8, containing 1 mM EDTA and 1 mM DTT; (—) myosin rod minifilaments in 5 mM sodium pyrophosphate buffer, pH 7.5, containing 1 mM EDTA and 1 mM DTT; (– · –) myosin rods in 50 mM sodium phosphate solution, pH 7.1, containing 0.6 M NaCl, 1 mM EDTA, and 1 mM DTT.

domain along the rod. The transition midpoints for minifilaments formed in 5 mM pyrophosphate (pH 7) solution are 40, 46.5, and 50 °C, respectively (Figure 9 and Table 3), which are 1–2 °C higher than those for rods at the same ionic strength. All of the structural domains are apparently involved in filament assembly since all three helix transition temperatures are higher for the filament than for soluble rods at the same ionic strength (Table 3). This result correlates with the fluorescence studies performed with probes in the S-2 and LMM regions, indicating that both proteolytic domains are involved in the formation of filaments (Table 2).

Three thermal unfolding transitions have been previously shown to occur for rabbit myosin rods in 0.6 M NaCl solution with transition midpoints of 43, 47, and 53 °C (King & Lehrer, 1989), while myosin rods in 5 mM pyrophosphate (pH 8) have transition midpoints of 37, 40, and 47 °C (Figure 10 and Table 3). From these 6–7 °C shifts in transition midpoints, it is suggested that high salt concentration stabilizes each structural domain of rabbit skeletal rods, similarly to chicken skeletal rods. Minifilament formation also stabilizes each structural domain along the rabbit skeletal rod. The transition midpoints for minifilaments formed in 5 mM pyrophosphate (pH 7) solution were 41, 44, and 49 °C (Figure 10 and Table 3), which are 2–4 °C higher than those for rods at an identical ionic strength.

The amino acid sequences of chicken and rabbit skeletal rods are similar, and the proteolytic susceptible sites are about the same for both proteins (Maita et al., 1991). Furthermore, our studies also demonstrate that chicken and rabbit skeletal rods have similar pressure dissociation properties. However, the thermal unfolding profiles of these two proteins are quite different from each other (Figures 9 and 10), suggesting a discrepancy in their cooperative structural domains and domain stabilities.

The thermal unfolding profiles of acrylodan-labeled gizzard rods exhibit two major transitions. Rods in 0.6 M NaCl have transitional midpoint temperatures of 48 and 53 °C, respectively, while rods in 5 mM pyrophosphate (pH 8) have transitional midpoints at 37.5 and 49 °C (Figure 11 and Table 3). High salt (0.6 M NaCl) stabilizes both rod domains, as judged by the 10.5 °C shift of the first transition temperature and the 4 °C shift of the second one. Rod minifilaments also have two thermal unfolding transitional midpoints at 41 and 50 °C (Figure 11 and Table 3), which are higher than those of the soluble rods at the same ionic strength. This result implies that the formation of filaments stabilizes both structural domains of gizzard rods.

Table 3: Thermal Helix Transition Midpoints (°C) of Myosin Rods and Rod Minifilaments

	rabbit rods	chicken skeletal rods			gizzard rods
	native	native	acrylodan on S-2	acrylodan on LMM	acrylodan on Cys-43
rods in 0.6 M high salt	43	44	44	43	48
	47	51	50	49.5	53
	53	55	55	54	
rods in 5 mM pyrophosphate	37	38	39	37	37.5
	40	45	45	43	49
	47	49	49	49	
minifilaments in 5 mM pyrophosphate	41	40	40	39	41
	44	46.5	46.5	45	50
	49	50	50	50	

The reversibility of thermal unfolding has been determined by a comparison of the unfolding and refolding profiles obtained by heating and cooling processes, respectively. Complete reversibility is achieved by initiating the cooling process immediately after the heating process. The larger discrepancy between folding and unfolding profiles could arise from longer incubation periods at high temperature. However, the original ellipticity was always recovered upon cooling to below 25 °C. The turbidity of the sample gradually increased when incubated at a high temperature. A higher temperature causes a faster increase in turbidity. These results suggest the occurrence of a slow aggregation process with a rise in temperature above a certain level.

The conclusions about the various regions of individual rod molecules participating in filament formation are as follows: (1) Both the tryptophan-containing region (near the N-terminal region of LMM) of skeletal rods and the Cys-43 region (near the head–rod junction region) of gizzard rods are involved in filament assembly, as indicated by the fluorescence probing. (2) Both LMM and S-2 regions of chicken skeletal rods participate in filament formation as suggested by the results of fluorescence probes labeled at each region. (3) Each of the cooperative structural domains of a rod participates in filament assembly, as substantiated from our thermal unfolding studies on myosin rods from three different sources. However, these studies on rods and rod minifilaments may not necessarily represent the same situation of myosin and thick filaments. In the case of myosin, the effect of the globular head on the conformation of rod structure and filament assembly cannot be ignored.

The ionic effects on structure and function of myosin have been thoroughly investigated (Warren et al., 1966; Stafford, 1985), and the results indicate that high salt (0.3–3 M) destabilizes the myosin structure and inhibits its ATPase activity. An extremely low ionic strength (5 mM pyrophosphate) may also destabilize the structure of myosin rods, as indicated from our studies on myosin rods from three different sources. Harrington (1971) proposed a molecular model involving a helix–coil transition of the "hinge" region (Tsong et al., 1979) of myosin rods, suggesting the presence of a region within the rod capable of unfolding at a temperature close to the physiological temperature. However, the lowest transition temperature we observed is 43 °C for a myosin rod in a conventional salt concentration (0.6 M). This nonphysiological ionic strength may account for the difficulty we encountered in observing the helix–coil transition at physiological temperature. The real transition temperature for this region at physiological ionic strength still remains uncertain despite the fact that a transition of myosin rods with a midpoint close to physiological temperature has been found in a solution of either an extremely high (>3 M NaCl; Stafford, 1985) or a very low ionic strength (5 mM sodium pyrophosphate).

In summary, the relevance of a proper ionic strength solution and the aggregation state on the structural and functional properties of myosin has been clearly demonstrated in previous studies (Warren et al., 1966; Stafford, 1985) and in this paper. Additionally, equilibrium disassembly of rod minifilaments by pressure has been established, which may be useful in the future to investigate filament assembly under physiological ionic strength. The use of a solution close to physiological conditions would be valuable in formulating models of force generation, of thick filament formation and replacement, and of some myosin-based regulatory systems of contraction.

ACKNOWLEDGMENT

The authors express their appreciation to Mr. G. C. Sheu and Ms. F.-L. Liang for technical assistance.

REFERENCES

Atkinson, S. J., & Stewart, M. (1991) *J. Cell Sci. 99*, 823–836.
Burke, M., Himmelfarb, S., & Harrington, W. F. (1973) *Biochemistry 12*, 701–710.
Cross, R. A., & Vandekerckhove, J. (1986) *FEBS Lett. 200*, 355–360.
Cross, R. A., Bardsley, R. G., Ledward, D. A., Small, J. V., & Sobieszek, A. (1984) *Eur. J. Biochem. 145*, 305–310.
Davis, J. S. (1988) *Annu. Rev. Biophys. Biophys. Chem. 17*, 217–239.
Davis, J. S., Buck, J., & Greene, E. P. (1982) *FEBS Lett. 140*, 293–297.
Dibb, N. J., Brown, D. M., Karn, J., Moerman, D. G., Bolten, S. L., & Waterston, R. H. (1985) *J. Mol. Biol. 183*, 543–551.
Ebashi, S. (1976) *J. Biochem. (Tokyo) 79*, 229–231.
Goodno, C. C., Harris, T. A., & Swenson, C. A. (1976) *Biochemistry 15*, 5157–5160.
Harrington, W. F. (1971) *Proc. Natl. Acad. Sci. U.S.A. 68*, 685–689.
Harrington, W. F., & Burke, M. (1972) *Biochemistry 11*, 1448–1455.
Harrington, W. F., & Rogers, M. E. (1984) *Annu. Rev. Biochem. 53*, 35–73.
Heremans, K. (1982) *Annu. Rev. Biophys. Bioeng. 11*, 1–21.
Hodge, T. P., Cross, R., & Kendrick-Jones, J. (1992) *J. Cell Biol. 118*, 1085–1095.
Holtzer, M. E., Holtzer, A., & Skolnick, J. (1983) *Macromolecules 16*, 173–180.
Huxley, H. E. (1969) *Science 164*, 1356–1366.
Josephs, R., & Harrington, W. F. (1966) *Biochemistry 5*, 3474–3487.
Josephs, R., & Harrington, W. F. (1967) *Proc. Natl. Acad. Sci. U.S.A. 58*, 1587–1594.
Josephs, R., & Harrington, W. F. (1968) *Biochemistry 7*, 2834–2845.
King, L., & Weber, G. (1986) *Biochemistry 25*, 3632–3637.
King, L., & Lehrer, S. S. (1988) *Biophys. J. 53*, 176a.
King, L., & Lehrer, S. S. (1989) *Biochemistry 28*, 3498–3502.
King, L., Lehrer, S. S., & Seidel, J. (1989) *Biophys. J. 55*, 77a.

Kumon, A., Kuba, M., Murakami, N., Yasuda, S., Takashima, T., Matsumura, S., & Suezaki, Y. (1986) *Eur. J. Biochem. 160*, 499–506.

Lakowicz, J. R. (1983) *Principles of Fluorescence Spectroscopy*, pp 341–379, Plenum Press, New York.

Lowey, S., Slayter, H. S., Weeds, A. G., & Baker, H. (1969) *J. Mol. Biol. 42*, 1–29.

Maeda, K., Sczakiel, G., & Wittinghofer, A. (1987) *Eur. J. Biochem. 167*, 97–102.

Maeda, K., Rosch, A., Maeda, Y., Kalbitzer, H. R., & Wittinghofer, A. (1991) *FEBS Lett. 281*, 23–26.

Maita, T., Nagata, S., Miyanishi, T., Yajima, E., & Matsuda, G. (1991) *Biophys. J. 59*, 228a.

Margossian, S. M., & Lowey, S. (1982) *Methods Enzymol. 85B*, 55–71.

McLachlan, A. D., & Karn, J. (1982) *Nature 299*, 226–231.

McLachlan, A. D., & Karn, J. (1983) *J. Mol. Biol. 164*, 605–626.

Nath, N., Nag, S., & Seidel, J. C. (1986) *Biochemistry 25*, 6169–6176.

Neuman, R. C., Jr., Kauzmann, W., & Zipp, A. (1973) *J. Phys. Chem. 77*, 2687–2691.

Nyitray, L., Mocz, G., Szilagyi, L., Balint, M., Lu, R. C., Wong, A., & Gergely, J. (1983) *J. Biol. Chem. 258*, 13213–13220.

Oriol-Audit, C., Lake, J. A., & Reisler, E. (1981) *Biochemistry 20*, 679–686.

Paladini, A. A., Jr., & Weber, G. (1981) *Rev. Sci. Instrum. 52*, 419–427.

Prendergast, F. G., Meyer, M., Carlson, G. L., Iida, S., & Potter, G. L. (1983) *J. Biol. Chem. 268*, 7541–7544.

Privalov, P. L. (1982) *Adv. Protein Chem. 35*, 1–104.

Reisler, E., Smith, C., & Seegan, G. (1980) *J. Mol. Biol. 143*, 129–145.

Reisler, E., Cheung, P., Borochov, N., & Lake, J. A. (1986) *Biochemistry 25*, 326–332.

Ruan, K., & Weber, G. (1988) *Biochemistry 27*, 3295–3301.

Ruan, K., & Weber, G. (1993) *Biochemistry 32*, 6295–6301.

Sreter, F. A., Holtzer, S., Gergely, J., & Holtzer, H. (1972) *J. Cell Biol. 55*, 586.

Stafford, W. F., III. (1985) *Biochemistry 24*, 3314–3321.

Tashiro, Y., Kumon, A., Yasuda, S., Murakami, N., & Matsumura, S. (1985) *Eur. J. Biochem. 148*, 521–528.

Tsong, T. Y., Karr, Y., & Harrington, W. F. (1979) *Proc. Natl. Acad. Sci. U.S.A. 76*, 1109–1113.

Ueno, H., & Harrington, W. F. (1981) *Proc. Natl. Acad. Sci. U.S.A. 78*, 6101–6105.

Warren, J. C., Stowring, L., & Morales, M. F. (1966) *J. Biol. Chem. 241*, 309–316.

Weber, G. (1986) *Biochemistry 25*, 3626–3631.

Weber, G. (1987) Dissociation of Oligomeric Proteins by Hydrostatic Pressure, in *Chemistry and Biochemistry at High Pressure* (van Eldyk, R., & Jonas, J., Eds.) NATO ASI Series C197, pp 401–420, D. Reidel, Dordrecht, The Netherlands.

Weber, G. (1991) Pressure and Temperature Stability of Oligomeric Enzymes, in *New Trends in Biological Chemistry* (Ozawa, T., Ed.) pp 225–238, Japan Scientific Society Press, Tokyo, and Springer, Berlin.

Weber, G. (1993) Relations of Bond Energies and Entropy with Volume, Pressure and Temperature in Protein Aggregates, in *High Pressure in Chemistry, Biochemistry and Material Science* (Winter, R., & Jonas, J., Eds.) NATO ASI Series C401, Kluwer, Dordrecht, The Netherlands.

Weber, G., & Farris, F. J. (1979) *Biochemistry 18*, 3075–3078.

Weber, G., & Drickamer, H. G. (1983) *Q. Rev. Biophys. 16*, 89–112.

Weeds, A. G., & Pope, B. (1977) *J. Mol. Biol. 111*, 129–157.

Xu, G.-J., & Weber, G. (1982) *Proc. Natl. Acad. Sci. U.S.A. 79*, 5268–5271.